EVALUATION OF CORRELATION CRITERIA FOR SAR IMAGES

Florence TUPIN, Michel ROUX, Saeid HOMAYOUNI

GET - Télécom-Paris - UMR 5141 LTCI - Département TSI
46 rue Barrault, 75013 Paris - France
¤orence.tupin@enst.fr

KEY WORDS: SAR imagery, radargrammetry, correlation

ABSTRACT

The aim of this paper is to study the use of cross-correlation for radargrammetric applications. Two other criteria derived from Mean Square Error analysis are proposed. These three criteria are studied using two sets of tests on real data (high resolution, one-look image of a semi-urban area). The £rst test is based on the analysis of the heights of a set of buildings (the heights being obtained using the thresholded disparities computed by one of the criteria). Then the performances are analyzed for each building using the available ground truth. The second test is based on the matching of a set of points. These points are manually associated and the displacement is compared to the one given by the matching criterion. Eventually, the ROC curves are computed to compare the 3 criteria in different situations.

1 INTRODUCTION

SAR images are nowadays widely used for Digital Elevation Model (DEM) production. The interferometric potential of the Synthetic Aperture Radar (SAR) data permits to obtain accurate DEM and the recent SRTM mission is a new proof of this capability. Nevertheless, SAR data are also able to produce height information using the classical stereo-vision principle (Rosen£eld, 1968). However, rather few works have been done in this domain (Toutin, 1995). One of the main dif£culties in radargrammetry is the matching step which associates the pixels of both images. Due to the speckle phenomenon, this step is particularly dif£cult with SAR images. The normalized centered cross-correlation coef£cient, which is widely used for optical images gives noisy results with SAR data. Among the proposed solutions, pre-processing like edge detection or post-processing like clever £ltering of the associated pairs can be used.

The aim of this paper is to analyze correlation criteria and study their behaviors when applied on real SAR images. We £rst describe 3 criteria which will be studied in the paper. Then we describe the two sets of tests that have been done to do the comparison. The £rst test is based on the analysis of the heights of a set of buildings (the heights being obtained using the thresholded disparities computed by one of the criteria). Then the performance are analyzed for each building using the available ground truth. The second test is based on the matching of a set of points. These points are manually associated and the displacement is compared to the one given by the matching criterion. Eventually, the ROC curves are computed to compare the 3 criteria in different situations.

2 URBAN SAR IMAGES AND RADARGRAMMETRY

SAR image interpretation in urban areas is known as very dif£cult task because of many phenomena: speckle, distance sampling, lay-over areas, and shadows. As pointed out in (Hardaway et al., 1982) (Tupin et al., 2002) the appearance of an object is strongly related to its geometrical properties in regards to the along track direction and the incidence angle. It is also depending on its roughness compared to the wavelength. Because of multiple bounce scatterings, many very bright features corresponding to dihedral or trihedral con£gurations are present in the data (Franceschetti et al., 2002). They correspond to wall / ground corners, balconies, chimneys, posts, street lamps, etc. Therefore SAR images in urban areas are usually composed of very bright features on a darker background with speckle. An example is shown in £gure 1. Since some roofs are quite smooth compared to the wavelength (9cm in S band), their mean radiometry is rather close to ground radiometry.

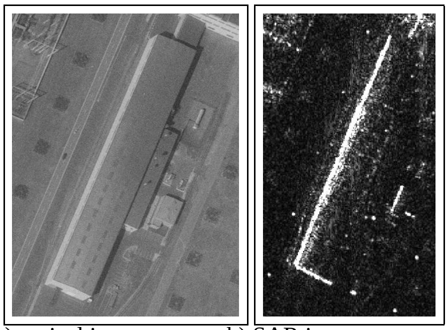

a) optical image   b) SAR image

Figure 1: Appearance of a building on the SAR image. Most of the information is given by very bright features (points or lines) corresponding to dihedral or trihedral con£gurations.

For these reasons, classical stereovision algorithms based on the correlation coef£cient between the two acquisitions are not very successful. The phenomenon has been observed for satellite data and therefore many £gural approaches have been developed for radargrammetric applications (Ansan and Thouvenot, 1995) (Marinelli et al., 1998) (Paillou and Gelautz, 1999). We study here the use of dedicated correlation measures adapted to multiplicative noise (Tupin, 2002).

3 CORRELATION CRITERIA

The problem to solve is to test the correspondence between two signals. In radargrammetric applications, the £nal purpose is to recognize if the £rst signal is present in the second one, each signal being a small part of the two images.

This £rst part is dedicated to the presentation of the three criteria that will be tested in the following of the paper. The £rst criterion is the classical normalized centered cross-correlation, widely used for optical images. The second one called “variation coef£cient criterion” has been proposed in a previous work (Tupin, 2002) and is a mixture of the classical cross-correlation coef£cient and the variation coef£cients (standard deviation normalized by the mean). The third one is a new criterion called “logarithmic criterion” in the following which is derived using the multiplicative noise model of the SAR images. These three criteria are de£ned in the following three sub-sections.

3.1 Cross-correlation criterion

The cross-correlation coef£cient is usually presented using a probabilistic approach. Let X_1 and X_2 be two real random variables, the centered normalized correlation ρ is de£ned by:

$$\rho = \frac{\mathrm{cov}(X_1, X_2)}{\sigma_1\sigma_2} = \frac{\mathrm{E}(X_1X_2) - \mu_1\mu_2}{\sigma_1\sigma_2} \tag{1}$$

with E the expectation, μ_i and σ_i the mean and standard deviation of X_i. It measures the linearity of the relationship between X_1 and X_2. For normalized centered random variables, it reduces to $\mathrm{E}(X_1X_2)$.

Having ρ de£ned by eq.1 and N real[1] samples of X_1 and X_2 denoted by x_{1i} and x_{2i} for $i \in \{1, ..., N\}$, there are many estimators $\hat{\rho}$ of ρ.

The moment estimator is given by:

$$\hat{\rho} = \frac{\frac{1}{N}\sum_i x_{1i}x_{2i} - \hat{\mu}_1\hat{\mu}_2}{\hat{\sigma}_1\hat{\sigma}_2} \tag{2}$$

with $\hat{\mu}_j = \frac{1}{N}\sum_i x_{ji}$ and $\hat{\sigma}_j^2 = \frac{1}{N}\sum_i x_{ji}^2 - \hat{\mu}_j^2$.

Another estimator which can be used to estimate the correlation coef£cient is the maximum likelihood (ML) estimator.

For the binormal distribution, the ML estimator is the same as the one obtained by the moment method and is given by eq.2 (Kendall and Stuart, 1969). The bias and variance of this usual sample correlation coef£cient can be derived in the case of binormal distribution assumption.

Another way of deriving the correlation coef£cient is the use of the Mean Square Error (MSE) to compare the X_1 and X_2 populations: MSE=$\mathrm{E}[(X_1 - X_2)^2]$. This quantity is minimized to search the best correspondence. To allow radiometric variations between the two signals, the MSE is applied to the centered normalized random variables which corresponds to MSE$= 2(1-\rho)$. Thus the minimization of the MSE for normalized random variables is equivalent to the maximization of the cross-correlation coef£cient.

[1] Note that in the case of SAR images, many different data can be used (complex £eld Z, intensity measure $I = |Z|^2$, amplitude data $A = |Z|$). There have been many works on the coherence estimation, specially in the interferometric framework addressing the interest of using complex or intensity data (Guarnieri and Prati, 1997) and studying the bias and variance of various estimators. But the aim is totally different in the radargrammetric context, since we are here interested in the correlation of the underlying scene of the 2 images. The speckle is for us de-correlated and thus a disturbing phenomenon, whereas in interferometry speckle is the “real” signal and the scene is the disturbing phenomenon (Guarnieri and Prati, 1997). Therefore, there is no interest in our context of using complex images instead of amplitude or intensity ones.

3.2 Variation coef£cient criterion

The probabilistic approaches which have been developed for SAR data strongly rely on scene and speckle assumptions. Since they are rarely veri£ed for un-natural areas, we preferred to use the Mean Square Error approach, to derive new criteria adapted to multiplicative noise. To keep the criterion increase in the case of a good match, we use the inverse of the MSE.

Using this idea, the criterion v has been derived keeping a radiometric difference to de£ne the error, but using a ratio based normalization and integrating the variation coef£cient γ_j of the random variables X_j to favor featured areas (Tupin, 2002):

$$1/v = \frac{\mathrm{E}[(\frac{X_1}{\mu_1} - \frac{X_2}{\mu_2})^2]}{\gamma_1\gamma_2} \tag{3}$$

In fact, we can see that v has also the following expression:

$$1/v = \frac{\gamma_1}{\gamma_2} + \frac{\gamma_2}{\gamma_1} - 2\rho$$

It means that this coef£cient has a global behavior similar to the one of the classical correlation, but tends to select windows with the same variation coef£cients (v is maximized when $\rho = 1$ and $\gamma_1 = \gamma_2$). This criterion is referenced as “variation coef£cient criterion” in the following.

It has been shown in (Tupin, 2002) using simulated data with theoretical Gamma distributions of different patterns and with different contrasts that:

- the variation coef£cient gives better results in terms of detection probability and false alarm rates on the original SAR data; results are only slightly better if a preliminary averaging is applied on the data;
- the localization accuracy of the match is better with the variation coef£cient criterion than with cross-correlation.

3.3 Logarithmic criterion

Since the speckle is modeled by a multiplicative noise (Goodman, 1975), a natural idea would be to use the logarithmic transformation to de£ne adapted criteria. A £rst test has been to apply the correlation coef£cient on logarithmically transformed images. But this criterion is not adapted to urban areas. Indeed, after logarithmic transformation, the small size bright targets are more dif£cult to detect. Since they are very important features in real urban scenes, the logarithm should not be used in practice.

Instead of using normalized centered variables $\frac{X-\mu}{\sigma}$ we propose to introduce the variable $X' = (\frac{X}{\mu})^\alpha$ and to de£ne the criterion by:

$$1/w = \mathrm{E}[(\log X_1' - \log X_2')^2] \tag{4}$$

Using the multiplicative noise model, $X = RS$ with R the scene re¤ectivity, and S the normalized speckle, with $\alpha = 1$ we obtain the following relationship (supposing that the two scenes are equal ($R_1 = R_2$):

$$\begin{aligned} 1/w &= \mathrm{E}[(\log \frac{R_1S_1}{\mathrm{E}(R_1)} - \log \frac{R_2S_2}{\mathrm{E}(R_2)})^2] \\ &= \mathrm{E}[\log \frac{S_1}{S_2}^2] \end{aligned}$$

This expression is not satisfying in a radargrammetric application since there is no way to distinguish homogeneous areas and pattern areas. Therefore, we introduced the scene variability in the α de£nition by taking:

$$\alpha = \frac{1}{\sqrt{\sigma^2 - \mu^2\sigma_S^2}}$$

σ and μ being the standard deviation and mean of the image (X), σ_S being the standard deviation of the speckle given by the look number of the SAR image ($\sigma_S = \frac{1}{\sqrt{L}}$ for intensity images). In this case, we have:

$$1/w \quad = \quad \frac{1}{\sigma_R^2(\sigma_S^2+1)}\mathrm{E}[(\log\frac{S_1}{S_2})^2] \qquad (5)$$

and the intrinsic variability of the scene is taken into account by the standard deviation of the scene σ_R.

3.4 Examples of application

An example to show the different behaviors of the three criteria is presented in £gures 2 and 3 for a punctual target. The “correlation images” are displayed which means that the correlation value for each displacement around the true match (in the center of the image) is displayed. It is a way to see the decreasing of the criteria around the good match and to see other maxima.

In £gures 4 and 5 another result is presented. This time, in each pixel the correlation value for the best match is displayed. As usual, the higher correlation values are obtained for patterns (specially the bright lines here).

A quantitative analysis is given in the two following sections using two HR SAR images on a semi-urban areas.

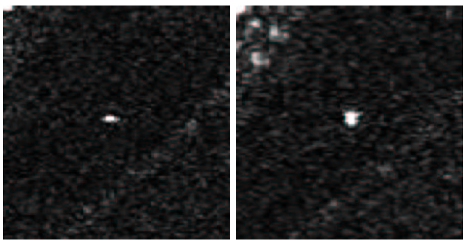

Figure 2: Left and right SAR images used for the correlation

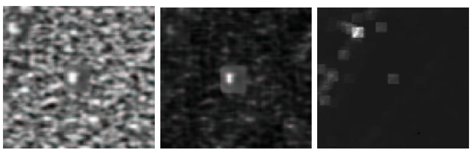

Figure 3: Correlation images for the three criteria: from left to right: values of cross-correlation coef£cient, the variation coef£cient criterion, and the logarithmic criterion.

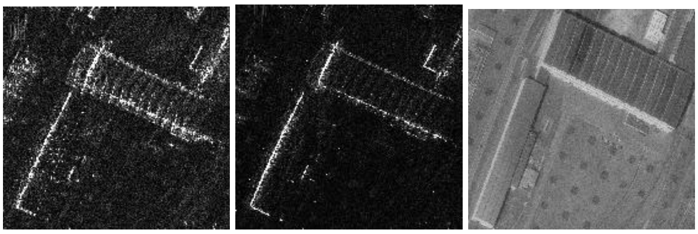

Figure 4: Left and right SAR images used for the correlation

A quantitative analysis is given in the two following sections using two HR SAR images on a semi-urban areas.

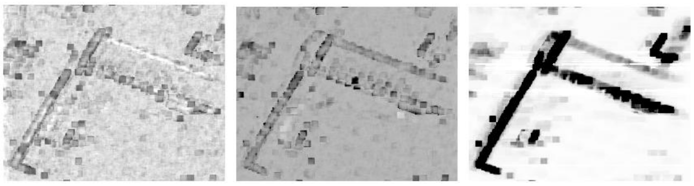

Figure 5: Correlation results for the three criteria: from left to right: cross-correlation coef£cient, variation coef£cient criterion, the logarithmic criterion (in negative display: the darker the pixel, the best the correlation value)

4 TEST ON BUILDING HEIGHTS

In this section, the comparison of the three criteria is done using a building map. For each building, we have a ground truth giving its true height (obtained by stereo-vision with optical images). For the SAR images, they are in epipolar geometry[2]. For each criterion, for each match above a £xed threshold, the associated disparity is converted in an height associated to the point.

The £rst step of this comparison is the study of the dynamic of each criterion to de£ne an adapted threshold. This value is of course crucial since it in¤uences the match selection. For the three criteria the value distributions have been empirically computed on a real SAR image. Then the mode of the probability density function has been selected, and will be used as a threshold value in the following tests. On the ground truth 10 buildings have been selected and subdivided into two sets: textured buildings and un-textured ones. We have used two criteria to study the performance of a correlator. The £rst criterion is the percentage of points which have been matched to the right height. The second criterion is the mean square error of the computed height (compared to the real one).

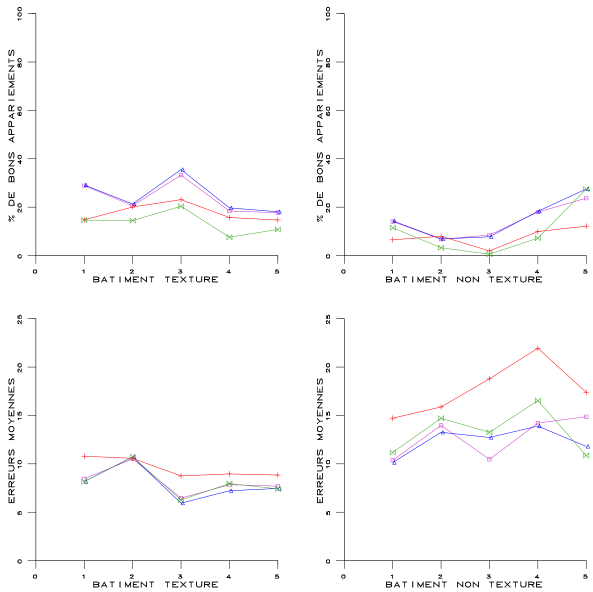

Figure 6: Percentage of good matchings (top) and mean square errors (bottom) for textured buildings (left) and untextured ones (right) for the three correlators (pink: cross-correlation; blue: variation coef£cient criterion; red: logarithmic criterion; green: fusion of the three correlators).

The fusion of the three correlators is done by selecting pixels for which the three matches are above the thresholds and giving the same disparity.

[2]Thanks to Thales for the epipolar geometry computation.

Using £gure 6, the following conclusions can be given:

- results are better for both criteria for the textured buildings and this is true whatever the correlator is;
- The two £rst correlators (cross-correlation and variation coef£cient criterion) have similar performances (with a slight advantage to the variation coef£cient criterion) whereas the logarithmic criterion is worst than the two other ones.

To complete this analysis, £gure 7 presents a classi£cation of the pixels depending on their accordance to the theoretical height of the building.

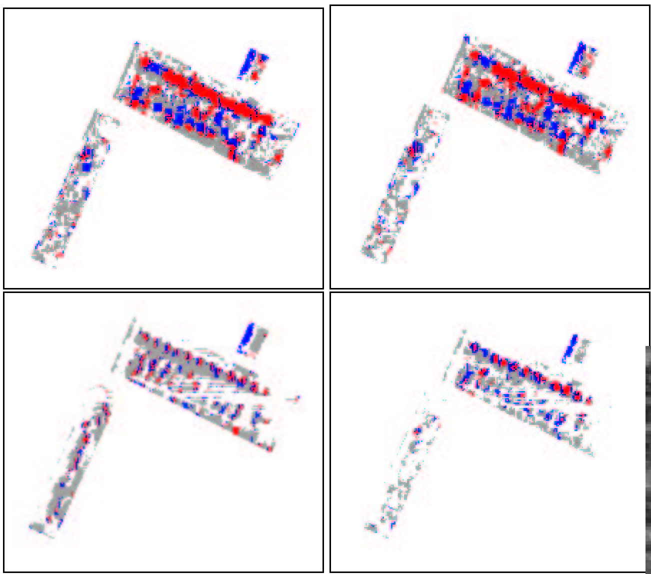

Figure 7: Colored classi£cation of the pixels depending on their error compared to the theoretical height (in red: with errors less than 2m; in blue: with errors less than 4m; in grey: with errors more than 4m -from top left to bottom right: cross-correlation, variation coef£cient criterion, logarithmic criterion, fusion of the three correlators-).

On this £gure 7, it seems that the logarithmic correlator gives right matches accurately located on the bright targets, whereas the two other ones give spread responses, thus increasing the percentage of well classi£ed pixels. This correlator is this more adapted to cross-shaped targets. This point is investigated in the second part.

5 TEST ON A SET OF POINTS

In this section, we are interested in the ROC curves computed for a set of manually selected points.

The test is done in the following way. The pair of points (P_1, P_2) in each image is selected manually. This selection is done in a very accurate way using visual criteria (contextual knowledge, etc.). Two sets of points have been de£ned. The £rst one correspond to bright punctual isolated targets and the second one to "L" shape corners (usually corresponding to ground/wall corner re¤ectors). For each point P_1 the best match in image 2 for a given correlation window and a given search area is computed. This match is localized in P_2' with value v. Three situations are considered for a given threshold th on the correlation value:

- if $d(P_2, P_2') \leq 2$ pixels and $v > th$: good detection;
- if $d(P_2, P_2') > 2$ pixels and $v > th$: false alarm;
- if $v \leq th$: point not taken into account.

Using these de£nitions, for each threshold on the correlation criterion, a probability of detection and a false alarm probability is computed. The ROC curves are then deduced for each criterion.

5.1 Results for the punctual bright targets

An example of a manually selected pair of points is shown on £gure 8. The results of the correlation values in the search area for a 9×9 window are presented £gure 9.

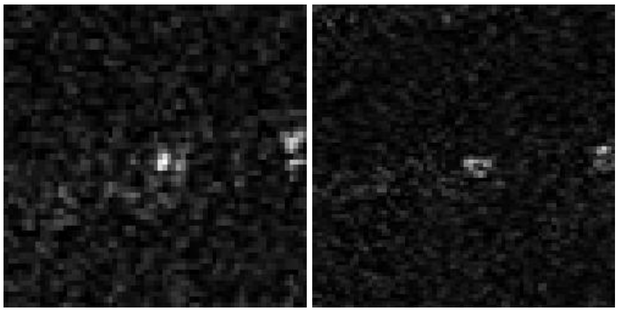

Figure 8: Pair of points manually selected in the two images (bright punctual target.

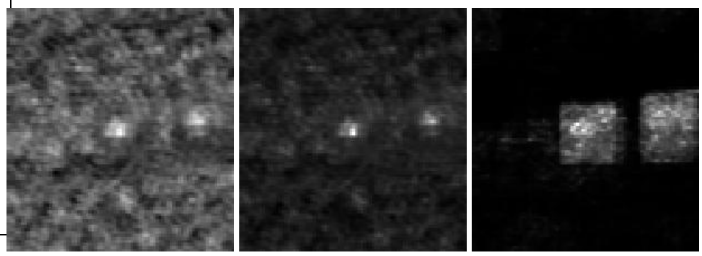

Figure 9: Correlation images for the three criteria (from left to right: cross-correlation, variation coef£cient criterion, logarithmic criterion) applied on the pair of £gure 8.

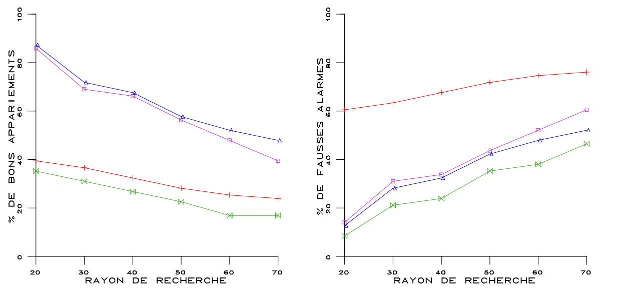

Figure 10: Percentage of good matchings (on the left) and false alarms (on the right) versus the size of the search area (in pink: cross-correlation; in blue: variation coef£cient criterion; in red: logarithmic criterion; in green: merged criterion).

Figure 10 shows the behavior of the 3 correlators when the search area is increased. As expected, the percentage of good matches decreases when the search area increases, whereas the false alarm percentage increases. A radius of 40 pixels for the search area has been eventually chosen to compute the ROC curves.

On this £gure, it can be observed that the variation coef£cient criterion has better performances than the others.

This result is con£rmed on the £gure 11 (ROC curves) showing that the best performance is obtained for the variation coef£cient criterion.

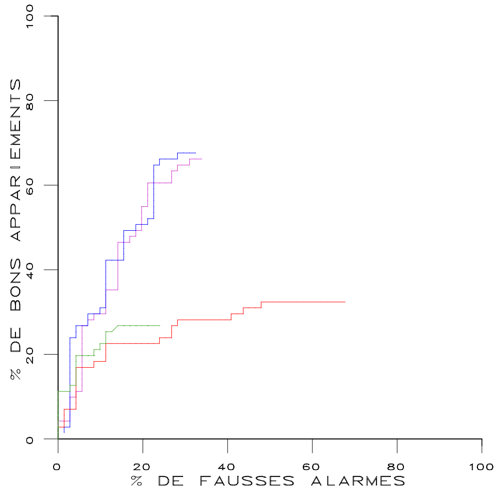

Figure 11: ROC curves for the punctual targets (in pink: cross-correlation; in blue: variation coef£cient criterion; in red: logarithmic criterion; in green: merged criterion).

5.2 Results for the "L" shape corners

Once again, an example of a manually selected pair of points in the set of "L shape" points is shown on £gure 12. The results of the correlation values in the search area for a 9×9 window are presented £gure 13.

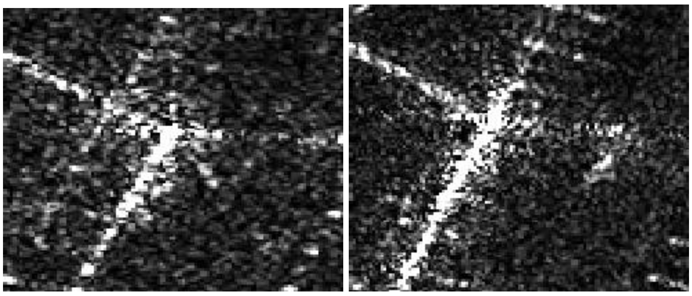

Figure 12: Pair of points manually selected in the two images ("L" shape corner).

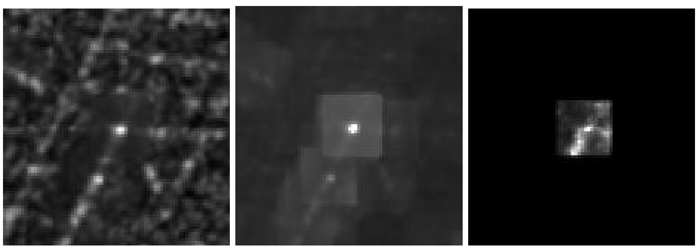

Figure 13: Correlation images for the three criteria (from left to right: cross-correlation, variation coef£cient criterion, logarithmic criterion) applied on the pair of £gure 12.

Once again, a radius of 40 pixels for the search area has been chosen.

For the case of "L-shape" pattern, the results are very different, since this time the best performances are given by the logarithmic criterion, whereas the variation coef£cient criterion gives the worst performances.

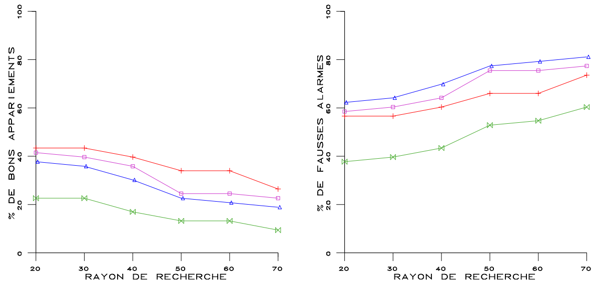

Figure 14: Percentage of good matchings (on the left) and false alarms (on the right) versus the size of the search area (in pink: cross-correlation; in blue: variation coef£cient criterion; in red: logarithmic criterion; in green: merged criterion).

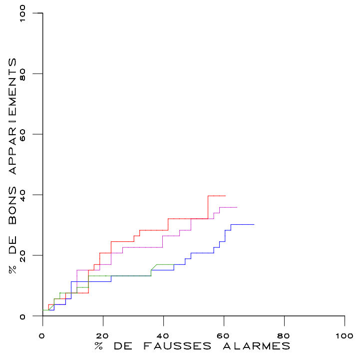

Figure 15: ROC curves for the "L-shape" targets (in pink: cross-correlation; in blue: variation coef£cient criterion; in red: logarithmic criterion; in green: merged criterion).

6 CONCLUSION

In this paper a new logarithmic based criterion has been proposed. A study of the behaviors of 3 correlators has shown that the performances depend on the kind of buildings on the one hand (£rst set of tests), and on the kind of considered targets (corners or punctual targets) on the other hand (second set of tests).

The best way to process SAR images would be to use the logarithmic criterion for "L shape" pattern and the variation coef£cient criterion for punctual targets, but to the price of a higher computational complexity.

Acknowledgment: The authors would like to thank Martin Hully for some algorithmic developments. Thanks also to ONERA and french DGA for providing the SAR images.

REFERENCES

Ansan, V. and Thouvenot, E., 1995. Semi-automatic stereoscopic radar image analysis. Europto 95, SPIE 2579, pp. 161–168.

Franceschetti, G., Iodice, A. and Riccio, D., 2002. A canonical problem in electromagnetic backscattering from buildings. IEEE Transactions on Geoscience and Remote Sensing 40(8), pp. 1787–1801.

Goodman, J., 1975. Statistical properties of laser speckle patterns. In: Laser Speckle and Related Phenomena, Vol. 9, J.C Dainty (Springer Verlag, Heidelberg, 1975), pp. 9–75.

Guarnieri, A. M. and Prati, C., 1997. SAR interferometry: A ”quick and dirty” coherence estimator for data browsing. IEEE Transactions on Geoscience and Remote Sensing 35(3), pp. 660–669.

Hardaway, G., Gustafson, G. and Lichy, D., 1982. Cardinal effects on Seasat images of urban areas. Photogrammetric Engineering and Remote Sensing 48(3), pp. 399–404.

Kendall, M. G. and Stuart, A., 1969. The Advanced Theory of Statistics. Vol. 1, 3 edn, Grif£n.

Marinelli, L., Laurore, L. and Poujade, V., 1998. A radargrammetry software for stereoscopic Radarsat images. ADRO Symposium, Montreal pp. 21–23.

Paillou, P. and Gelautz, M., 1999. Relief reconstruction from SAR stereo pairs: the ”optimal gradient” matching method. IEEE Transactions on Geoscience and Remote Sensing 37(4), pp. 2099–2107.

Rosen£eld, G. H., 1968. Stereo radar techniques. Photogrammetric Engineering pp. 586–594.

Toutin, T., 1995. Airborne SAR stereo restitution in a mountainous area of Costa Rica: £rst results. IEEE Transactions on Geoscience and Remote Sensing 33(2), pp. 500–504.

Tupin, F., 2002. Matching criteria for radargrammetry. In: IGARSS 2002, Vol. 5, Toronto, Canada, pp. 2608–2610.

Tupin, F., Houshmand, B. and Datcu, M., 2002. Road detection in dense urban areas using SAR imagery and the usefulness of multiple views. IEEE Transactions on Geoscience and Remote Sensing 40(11), pp. 2405–2414.